

Measured Energy and Angular Distributions of Sputtered Neutral Atoms from a Ga-In Eutectic Alloy Target

A.W. Bigelow¹, S.L. Li, S. Matteson, D.L. Weathers

University of North Texas, Denton, Texas

The energy and angular distributions of ground-state neutral atoms sputtered from the surface of a liquid Ga-In eutectic alloy by normally-incident 25 keV Ar⁺ have been measured using the technique of sputter-initiated resonance ionization spectroscopy (SIRIS). Details of the measurements and data analysis are presented. Differences between the distributions for the Ga and In atoms are discussed in the context of the extreme Gibbsian segregation of the alloy surface.

INTRODUCTION

Sputtering, a process of material erosion by particle bombardment, plays a significant role in many technologies, including integrated circuit manufacture and materials characterization techniques. In this study, the energy and angular distributions of neutral atoms sputtered from a multi-layered surface, a liquid Ga-In eutectic alloy, were measured. These results are useful for comparison with and possible further refinement of analytical and computational sputtering models. The reported distributions were measured using sputter-initiated resonance ionization spectroscopy (SIRIS), a technique for analyzing materials through selective resonance ionization of secondary neutral atoms.

Liquid Ga-In eutectic alloy is very well suited as a target to study the energy distribution of sputtered neutral atoms. Gibbsian segregation at the surface of the material results in an extreme concentration ratio gradient between the top two atomic layers. Previous studies have shown that the surface of the liquid Ga-In (16.5 at% In) eutectic is ≈ 94 at% In, and that this enhancement is almost exclusively in the top monolayer [1, 2]. The sputtering fraction from the first layer has been calculated to be 0.88 for a primary Argon ion beam energy of 25 keV [1]. Using the

values from this study, one can estimate that the fraction of In sputtered from the top layer is >0.98 . A corresponding estimate predicts that the fraction of Ga atoms sputtered from beneath the top monolayer is 0.75. This suggests, therefore, that the In energy distribution is dominated by atoms sputtered from the surface atomic layer. Likewise, any measurements of the energy distributions for Ga favor atoms sputtered from beneath the surface. The Ga-In liquid target also eliminates the dependence of sputtering on projectile fluence. With a liquid target, as sputtering continues, the surface layer and concentration gradient persist due to the high atomic mobility in the target.

EXPERIMENT

Components of the SIRIS machine at the University of North Texas (UNT) include a low-energy particle accelerator to provide a primary sputtering ion beam, an ultra-high vacuum target chamber, a tunable dye laser system for resonance ionization, and a position-sensitive detector. A time-of-flight detection method, initiated by a short pulse of primary ions on the sample and terminated by a resonance ionization laser pulse at the entrance to the detector, permits velocity measurements of the resonantly ionized particles. Fast timing electronics and data acquisition are handled through a virtual instrumentation program. Details of the

¹ Present address: Center for Radiological Research, Columbia University, New York, NY 10024, USA.

instrumentation are documented in a previous article [3]. The SIRIS apparatus cycles at 10 Hz. A schematic representation of the detector is shown in fig. 1. The sample orientation in the figure represents that used in this work. Individual photoions impinging on the detector's microchannel plates ultimately produce scintillations on a phosphor screen that are recorded by a charged coupled device (CCD) camera.

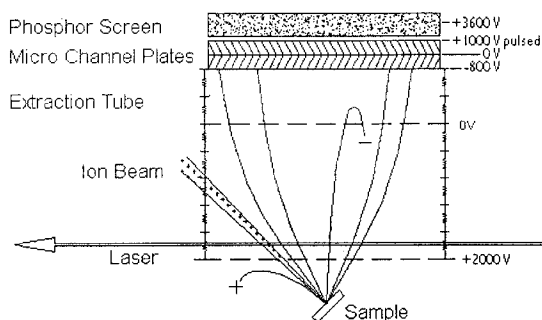


FIGURE 1. Schematic diagram of the interaction region and the position-sensitive detector. Dashed lines represent high-transmission grids.

The Ga-In eutectic alloy target material was obtained commercially. Appropriate handling of such material, which is liquid at room temperature, has been previously documented [4]. Two attributes of the liquid Ga-In eutectic alloy allowed for vertical mounting inside a vacuum system. In past experiments, the eutectic exhibited good wetting without dissolution on cobalt [5]. In addition, the eutectic has a low vapor pressure, rated as essentially zero by the manufacturer [6]; hence, it will not evaporate in a UHV environment. The sample was cleaned in a nitrogen back-filled glove bag attached to the sample introduction port. In this environment, the Ga oxide film layer that is known to form on the Ga-In eutectic [2] was swept off with a small wire brush.

To measure the energy distribution of sputtered neutral atoms, a series of different flight times for the atoms to reach the photoionization region was selected. Each time corresponded to a particular component of sputtered particle energy in the direction normal to the face of the detector. For Ga, the energy series comprised 1, 3, 5, 7.5, 10, 12.5, 15, 20, 25, 30, 35, and 40 eV. For In, the chosen energies were 1, 3, 4, 5, 6, 7.5, 10, 15, and 20 eV. Different energies were used for Ga and In because of differences in the energy distributions for the two different species. Data acquisition involved integrating a CCD image over many apparatus cycles to capture an overall intensity distribution built from successive individual ion impacts.

For each element, the primary sputtering ions were 25 keV Ar in a pulsed beam with pulse widths of 200 ns. The amplitudes of the ion pulses and the average laser power were recorded for data normalization. Typical instantaneous ion beam current was 100 nA and typical average laser power was 20 mW for Ga and 8 mW for In. In both cases, these laser power averages included a fundamental and a second harmonic wavelength. A BBO crystal used to double the dye laser output was measured to have 10% efficiency for second harmonic generation. Resonance ionization schemes exist for both Ga [7] and In [8]. The wavelengths chosen for Ga ionization were 287.4 nm for resonance and 574.8 nm for photoionization. For In, the chosen wavelengths were 303.9 nm for resonance and 607.8 nm for photoionization.

RESULTS

All ion impact positions on the CCD images were convolutions of particle energy and angle; image processing was required before final distributions of sputtered neutrals could be obtained. The first step in the processing of the raw data images was to extract the gray-scale pixel values representing particle impact intensity vs. position. The data were normalized with respect to the number of incident primary ions. The In data were also normalized to average laser power because the photoionization was linearly dependent on power in this case. A correction for spatial efficiency fluctuations across the microchannel plates and phosphor screen was required. Particle impact positions were then translated into initial ejection energies and angles. Sets of these data were expressed in terms of differential sputtering yields. The next figures illustrate the data processing steps for the 5 eV Ga measurement. They are followed by data set compilations and energy and angular sputtering distributions. Figure 2 depicts one of the images of acquired intensities at the 5 eV Ga setting.

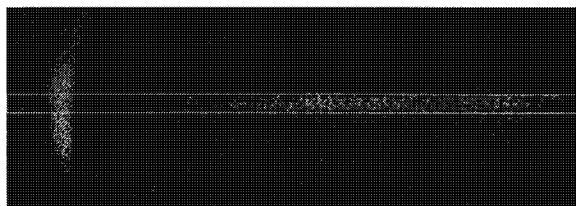


FIGURE 2. An image of SIRIS signal with the dynamic data exchange region of interest. Laser-induced stray-light background effects are responsible for the intensity arc on the left.

Figure 3 shows signal intensity averaged over three individual images. Such an average accounts for 18,000 apparatus cycles. All data were acquired and compiled in this fashion.

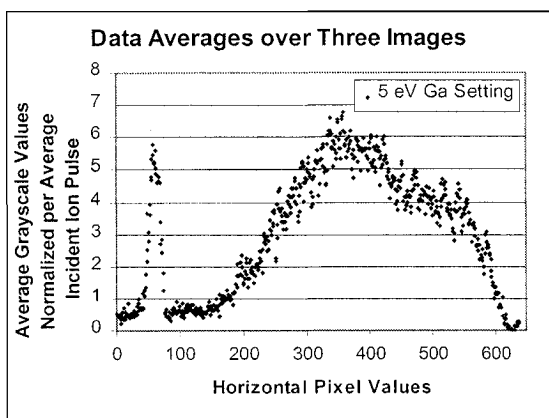


FIGURE 3. SIRIS signal averaged over three integrations with identical experimental parameters.

Following spatial efficiency correction, the modified image intensities for the 5 eV Ga setting are shown in fig. 4. These data were fit with a sixth order polynomial function. The sixth-order fit was used for subsequent deconvolution of the data.

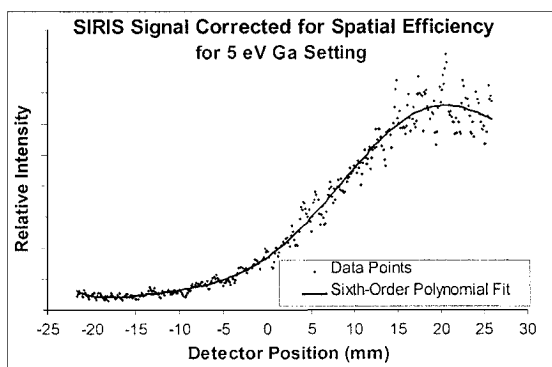


FIGURE 4. SIRIS data corrected for spatial efficiency of detector. The detector position axis range has been cropped to correspond to the angular emission range of interest: 0-85 degrees from sample normal.

Total kinetic energy for each sampled particle was calculated in a straightforward fashion once the ejection angles were known. To verify the correspondence between detector position and ejection angle, a series of images were acquired for which the range of ejection angles was truncated by a physical

shield. These results were compared with computer simulations of particle trajectories through the detector and with analytical expressions for the particle trajectories. After the sputtering data were converted from impact positions to unique ejection angles and energies, the image intensity was converted to a differential sputtering yield with respect to energy and angle. The differential sputtering yield for the 5 eV Ga setting is plotted in fig 5.

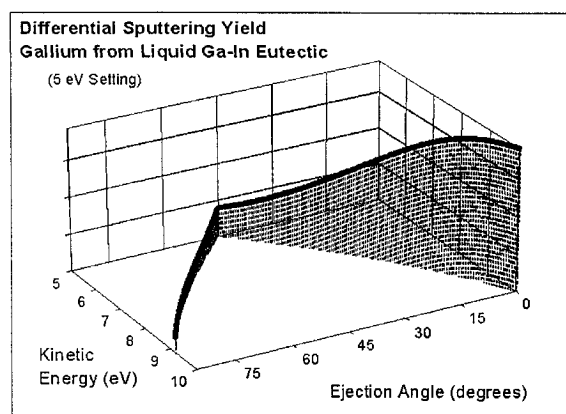


FIGURE 5. The differential sputtering yield with respect to energy and angle. This representation exhibits the image position deconvolution into angle and energy.

The differential sputtering yield, $\frac{dY}{dEd^2\Omega}(E, \theta)$,

is shown in a three-dimensional surface plot in fig. 6. In contrast, the In data formed a similar plot but were broader in angle and narrower in energy.

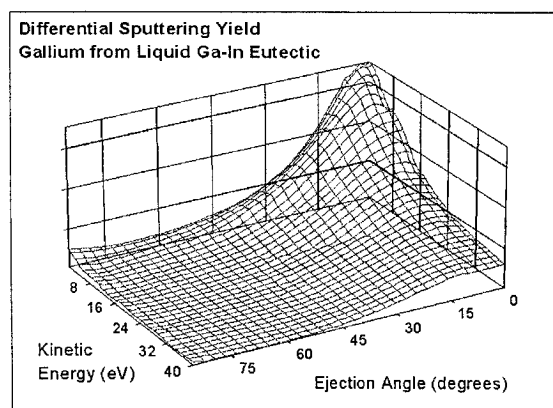


FIGURE 6. Grid plot of the differential sputtering yield with respect to energy and angle for Ga sputtered from liquid Ga-In eutectic alloy. The grid surface helps to visualize the energy peak in the distribution.

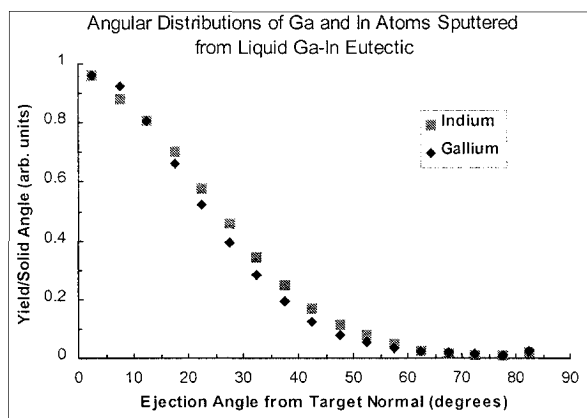


FIGURE 7. The angular distributions of sputtered Ga and In atoms from liquid Ga-In eutectic.

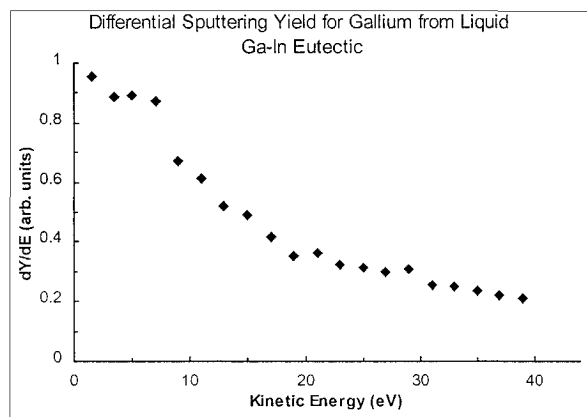


FIGURE 8. The energy distribution of sputtered Ga atoms from liquid Ga-In eutectic alloy.

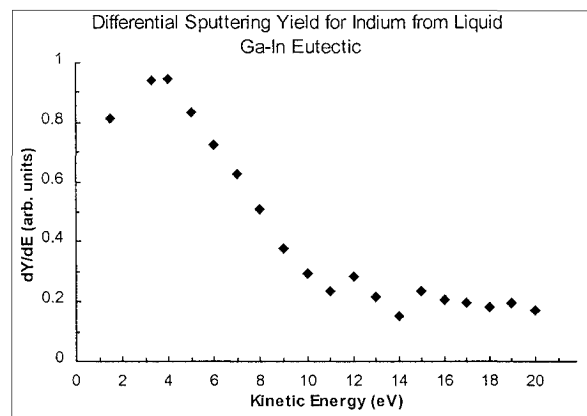


FIGURE 9. The energy distribution of sputtered In atoms from liquid Ga-In eutectic alloy.

Measured energy and angular distributions of sputtered neutral atoms from Ga-In eutectic alloy are displayed in fig. 7-9. For In, the trends are characteristic of sputtering from the top layer of a sample: the In yields are broader in angle and concentrated at lower energies than for Ga, which originates primarily from beneath the first monolayer. The angular distributions are consistent with the view that atoms originating from beneath the surface monolayer are less likely to escape in oblique directions because of a larger collision probability with the surface atoms in those directions. The energy distributions are consistent with the idea that the surface monolayer represents a barrier that prevents low-energy atoms from escaping from beneath the surface. Moreover, these results are in qualitative agreement with other angular measurements [1, 2] and with the results from molecular dynamics simulation [9]. Quantitative differences could be due in part to the coarseness of the sampling in the measurements reported here.

ACKNOWLEDGMENTS

This work was supported in part by the Texas Advanced Research Program under Grant No. 003594-068.

REFERENCES

1. K.M. Hubbard, R.A. Weller, D.L. Weathers, T.A. Tombrello, *Nucl. Inst. and Meth.* **B 36**, 395 (1989).
2. M.F. Dumke, T.A. Tombrello, R.A. Weller, R.M. Housley, and E.H. Cirlin, *Surface Sci.* **124**, 407 (1983).
3. A.W. Bigelow, S.L. Li, S. Matteson, D.L. Weathers, "Sputter-Initiated Resonance Ionization Spectroscopy at the University of North Texas," in *Appl. of Accel. in Res. and Ind.*, ed. by J.L. Duggan and I.L. Morgan, AIP Conf. Proc. 475, New York, 1999, pp. 569-572.
4. K.M. Hubbard and R.A. Weller, *Surface Sci.* **207**, 441 (1989).
5. T.B. Lill, W.F. Callaway, M.J. Pellin, and D.M. Gruen, *Phys. Rev. Lett.* **73** 12, 1719 (1994).
6. Alfa Aesar, Material Safety Data Sheet.
7. E.B. Saloman, *Spectrochimica Acta* **49B** 3, 251 (1994).
8. E.B. Saloman, *Spectrochimica Acta* **48B**, 1139 (1993).
9. M.H. Shapiro, K. Bengtson, Jr., and T.A. Tombrello, *Nucl. Inst. and Meth.* **B 103**, 2 (1995).